Reversible, Nanometer-Scale Conductance Transitions in an Organic Complex

H. J. Gao,[1,2] K. Sohlberg,[1] Z. Q. Xue,[2] H. Y. Chen,[2] S. M. Hou,[2] L. P. Ma,[2] X. W. Fang,[3] S. J. Pang,[2] and S. J. Pennycook[1]

[1]*Solid State Division, Oak Ridge National Laboratory, P.O. Box 2008, Oak Ridge, Tennessee 37831-6031*
[2]*Beijing Laboratory of Vacuum Physics, Institute of Physics and Center for Condensed Matter Physics, Chinese Academy of Sciences, Beijing 100080, People's Republic of China*
[3]*Department of Biochemistry and Molecular Biology, University of Chicago, Chicago, Illinois 60637*
(Received 23 June 1999)

Reversible conductance transitions are demonstrated on the molecular scale in a complex of 3-nitrobenzal malononitrile and 1,4-phenylenediamine, by application of local electric field pulses. Both macroscopic and local current-voltage (I/V) measurements show similar electrical bistability behavior. The mechanism of the electrical bistability is discussed.

Conjugated organic materials have aroused much attention recently [1]. Of particular interest is the utilization of individual molecules or molecular complexes as electronic device elements. Aviram *et al.* [2] proposed the donor-bridge-acceptor (D-Σ-A) model for molecular rectification using conjugated molecules. A crucial issue in this regard is whether or not a conductance transition can be induced in single molecules or nanoscale regions of a thin film, and the mechanism of the transition. The pioneering work of Aviram *et al.* [3] reported the first evidence of switching and rectification in an organic thin film, but the results were not conclusive [4]. More recently, Potember *et al.* [5] have shown a field-induced conductance transition on a 500 nm scale, but did not demonstrate *local* reversibility. The reverse transition was induced only by application of a broad laser pulse or heat. Here we report a *reversible* conductance transition in a crystalline fully organic complex, on a scale close to the dimensions of the unit cell.

The two conjugated organic compounds shown in Fig. 1, 3-nitrobenzal malonitrile (NBMN) and 1,4-phenylenediamine (pDA), were used to form the complex. NBMN was prepared as in the literature [6], and the two materials were mixed together in a 1:1 molar ratio and vacuum evaporated (10^{-6}–10^{-5} Torr). High resistivity polycrystalline NBMN-pDA films were prepared by evaporation onto room temperature substrates at a rate ≤ 5 nm/min. Films for conductance transition experiments were deposited to a thickness of 20 nm on freshly cleaved, highly oriented pyrolytic graphite (HOPG). Samples for macroscopic four-probe I/V measurements were deposited to a thickness of 200 nm on substrates of glass coated with conductive indium-tin-oxide films. For transmission electron microscopy (TEM), films were simultaneously deposited onto carbon films and subsequently examined in a JEOL 200CX. Coverage was found to be very uniform. X-ray diffraction showed the polycrystalline films to have a triclinic structure with unit cell parameters: $a = 0.7823(2)$ nm, $b = 0.8730(2)$ nm, $c = 0.7286(1)$ nm, $\alpha = 105.90(3)°$, $\beta = 101.49(3)°$, $\gamma = 78.75(3)°$. In contrast, for deposition rates >6 nm/min, the resulting films were

conductive, and structural characterization showed these more rapidly deposited films to be amorphous. As discussed below, this result is a clue to the mechanism of the conductance transition.

We first performed standard four-point probe measurements of *I-V* relationships and transient conductance on the 200 nm thick films. The *I-V* measurements, shown in Fig. 2(a), demonstrate electrical bistability. Increasing the voltage stepwise from zero produced the open points in Fig. 2(a), but when the voltage was increased above 3.2 V, the film abruptly switched to a conductive state. In the conductive state, stepwise sampling of the current as a function of applied voltage produced the solid points in Fig. 2(a). The high-impedance state has a resistivity of $\approx 10^{-8}$ $\Omega \cdot$ cm, reducing to $\approx 10^{-4}$ $\Omega \cdot$ cm in the conductive state. We note that our films are significantly more conductive than those reported by Alvarado *et al.* [7]. The transition time of the film was measured to be about 80 ns, as shown in Fig. 2(b).

Local conductance transitions were induced in the high-resistivity films by a scanning tunneling microscope (STM). A typical image of the film is shown in Fig. 3(a). The dimensions of the surface unit cell are $b = 0.93$ nm, $c = 0.78$ nm, and the angle between $\hat{b}$ and $\hat{c}$ is about 100°, closely matching the unit cell dimensions determined by x-ray diffraction. This image was taken at a bias (V_b) of 0.1 V and tunneling current (I_t) of 0.4 nA. As shown in Figs. 3(b) and 3(c), a 3×3 array and an "A"
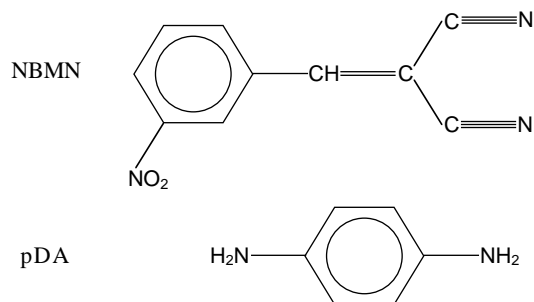

FIG. 1 Structures of the conjugated molecules NBMN and pDA.
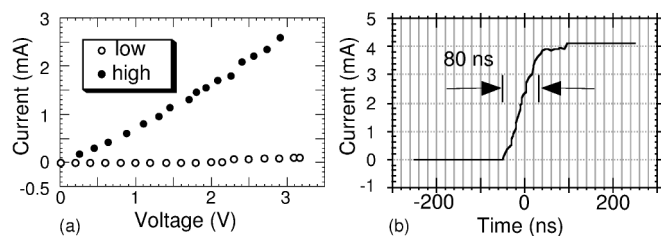
FIG. 2   (a) *I-V* relation of a 200 nm film, showing the low and high conductance states. The voltage threshold is 3.2 V. (b) Transient conductance measurements on the 200 nm film showing a transition time of 80 ns.

pattern could be formed by applying voltage pulses to the STM tip in constant height mode. Each bright spot in the image represents a high-conductance region, i.e., regions that have been switched from insulator to conductor. The shadow effect on each mark is due to the fact that the feedback circuits were not completely nulled during the
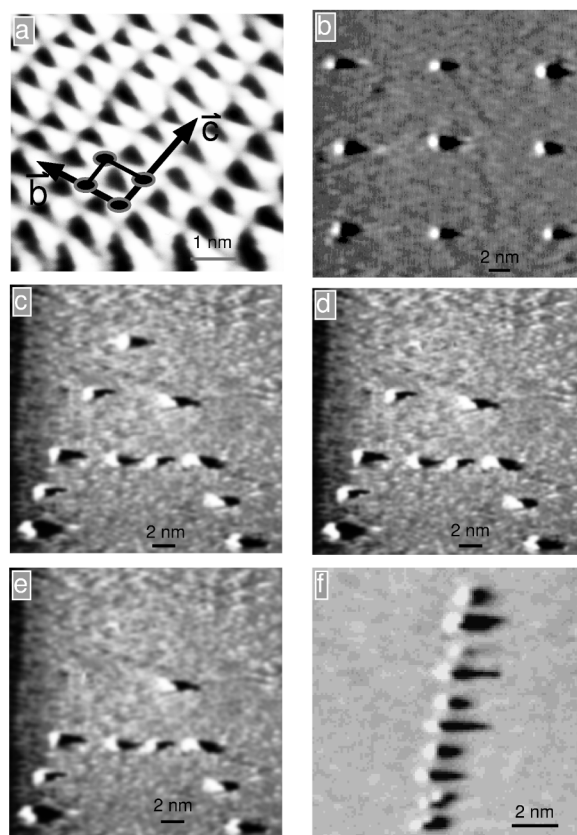

FIG. 3   STM images of the NBMN-pDA film on HOPG. (a) An image of the surface of the film showing crystalline order, image size: 6 nm × 6 nm; (b) a 3 nm × 3 nm array formed by voltage pulses of 4 V and 1 μs; (c) an "A" pattern formed by voltage pulses of 3.5 V and 2 μs; (d) and (e) STM images after erasing marks one at a time with reverse-polarity voltage pulses of −4.5 V and 50 μs; (f) resolution test using voltage pulses of 4.2 V and 10 μs. The distance between neighboring marks is 1.7 nm. Scan conditions are $V_b = 0.1$ V, $I_t = 0.4$ nA for (a); and $V_b = 0.19$ V, $I_t = 0.19$ nA for (b), (c), (d), (e), and (f); constant height mode.

scan. All marks were erased on heating the sample *in situ* above 423 K, when the conductance of the local regions recovered their original insulating states. It was possible to induce the reverse transition in *individual* marks by applying a reverse-polarity voltage pulse of −4.5 V for 50 μs, as shown in Figs. 3(d) and 3(e). If the same pulse was applied without reversing the polarity, the mark was incompletely erased. Therefore the process is due to the combined effect of applied field and a local heating induced by the current passing through the conducting region. In principle, the ultimate resolution should be the size of the molecular complex, ≈ 1 nm. Figure 3(f) demonstrates resolution on this length scale. The marks are separated by approximately 1.7 nm.

Finally, local *I-V* characteristics of the film measured before and after mark formation confirm the conductance transition. As shown in curve *a* of Fig. 4, with the NBMN-pDA in its initial high-impedance state, the applied voltage can be varied from 0 to 2.1 V but the tunneling current remains small (about 0.2 nA). Beyond a threshold of 2.1 V, the film changes to a low-impedance state with the *I-V* relation of curve *b*. Curve *b* clearly demonstrates conductivity and eliminates deposited charge as a possible mechanism of the mark formation. For comparison, the *I-V* curve from the graphite substrate is shown in curve *c* of Fig. 4. The *I-V* relation for the substrate is inconsistent with that of the film in its conducting state, eliminating the possibility that the conducting state is reached by simply burning a hole through the film.

Several possible mechanisms for the conductance transition were considered resulting in the identification of a candidate mechanism that is in agreement with all available experimental data for this system. The first candidate considered was the charge transfer (ct) mechanism proposed by Ma *et al.* [8] for conductance transitions in a thin organic film of N-(3-nitrobenzylidene)-*p*-phenylenediamine (NBPDA). In the ct mechanism, hypothetically, a voltage pulse above some threshold brings about a shift in
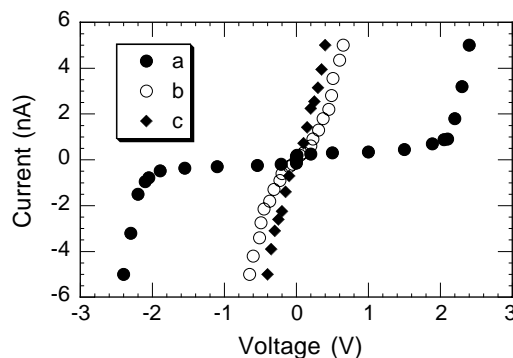

FIG. 4   Typical STM current-voltage relations. Curve *a*: Before the voltage pulse, with the film in a highly insulating state, which becomes conductive above a voltage threshold of 2.1 V; Curve *b*: *I-V* relation after the voltage pulse, indicating a transition to the conductive state; Curve *c*: linear *I-V* relation from the HOPG substrate.

electron density into a charge-separated state. While such an excited electronic state could presumably impart conductance properties to the molecule different from those of the ground state, in the present case, the ct mechanism is excluded by the transition time measurements. As shown in Fig. 2(b), the transition time from the initial high-impedance state to the conducting state is about 80 ns, many orders of magnitude longer than even the most sluggish of molecular electronic transitions. Furthermore, it is highly unlikely that an appreciable population could be sustained in the excited (ct) state for the hours to days that the film remains in the conducting state [8].

As a second possible mechanism it was considered that the individual molecular complexes of NBMN-pDA might undergo an internal rotation into an excited molecular conformation whose geometry completes the conjugated π structure *across the entire complex*. This is essentially the "conformational switching" mechanism of Joachim and Launay [9]. In a molecule containing two or more benzene rings in sequence, the electrical resistance increases by about $\times 10^4$ when the angle between the planes of adjacent rings is changed from 0 to 90° [10]. In the present case, the individual components contain extended π-conjugated structures. If these components were brought into alignment in an excited conformation, completing the π structure across the entire complex, it would result in greatly enhanced conduction in the excited conformation.

The present system proved too large to test the conformational isomerization hypothesis computationally, but we were able to carry out electronic structure calculations on a closely related system that exhibits the same electrical bistability behavior. Local conductance transitions have been demonstrated on the nanometer scale in NBPDA in the same laboratory as the present work [8]. The structure of NBPDA is shown in Fig. 5 (inset). We searched for stable conformations of this molecule at the Hartree-Fock/SCF level of theory [11]. Earlier calculations at this level resulted in excellent accuracy for both structure and intramolecular conformational energy differences in two conjugated organic systems similar to NBPDA [12]. As shown in Fig. 5, NBPDA exhibits two stable conformers. The predicted harmonic vibrational frequencies for the more stable of these two conformers reproduce the dominant peaks and features of the FTIR spectrum of crystalline NBPDA very well [13]. In both conformers, however, the two benzene rings are coplanar. Since the π-π conjugation extends over the entire NBPDA system in both conformers, we conclude that local conductance transformations observed in NBPDA do not arise from conformational isomerization, and by analogy it seems highly unlikely that such a mechanism would be at the root of the same phenomena in the very closely related NBMN-pDA system.

The most likely source of the local conductance transition in NBMN-pDA thin films is a mechanism whereby the applied electric pulse leads to a reorientation of one or
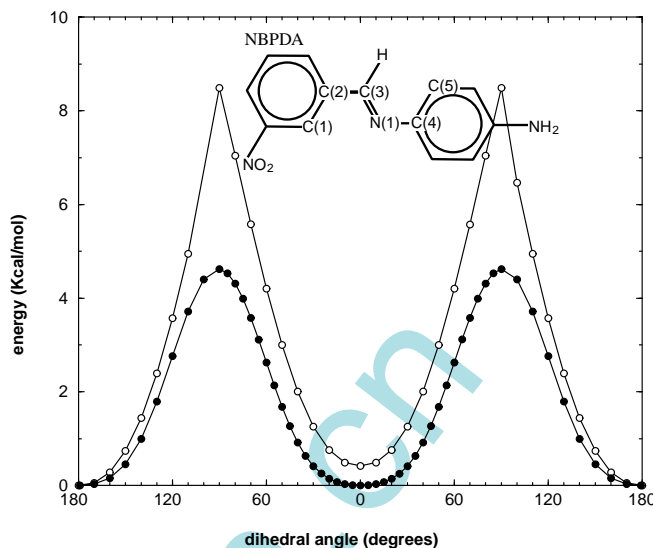

FIG. 5   The molecular structure of NBPDA (inset) and potential energy curves for internal rotations of NBPDA. Solid circles: rotation about the $(C_{(3)}, N_{(1)}, C_{(4)}, C_{(5)})$ dihedral angle. Open circles: rotation about the $(C_{(1)}, C_{(2)}, C_{(3)}, C_{(5)})$ dihedral angle.

more *entire molecules,* in effect introducing local disorder into the crystalline thin film. The experiments demonstrate that the crystalline films are insulating and the amorphous films are relatively conducting. This result is less surprising when one notes that this is an organic system, and carbon, while an excellent insulator when in the form of diamond, is much more conducting in various less-ordered forms. It follows naturally that if a local area of the film is structurally disordered, that region will become conducting. Since the NBMN-pDA system has a permanent dipole, an electric field pulse could lead to molecular reorientation. Such a reorientation would effectively introduce local disorder into the film. This "induced local disorder" hypothesis is also consistent with the mechanism for erasure. Only reversed polarity pulses completely reverse the conductance transition, and they must be applied for a longer duration than the "write" pulse. Obviously, if the "write" pulse grabs the permanent dipole and twists the molecule in one direction, reversing the twist will require the application of force of the opposite sign. Furthermore, the duration must be sufficient to allow time for the order to redevelop. Finally, the 80 ns characteristic transition time for the conductance transition, although much too slow for an electronic or conformational transition, is perfectly reasonable for *reorientation* of a large molecule. To test the hypothesis that the conductive region of the film is disordered, TEM and electron-diffraction studies were carried out on a film before and after switching. The results are shown in Fig. 6. As anticipated, the nonconductive film is crystalline, but after switching to the conductive state, the TEM and diffraction studies indicate an amorphous film.

In summary, we have demonstrated that conductance transitions can be induced by a local electric field in the
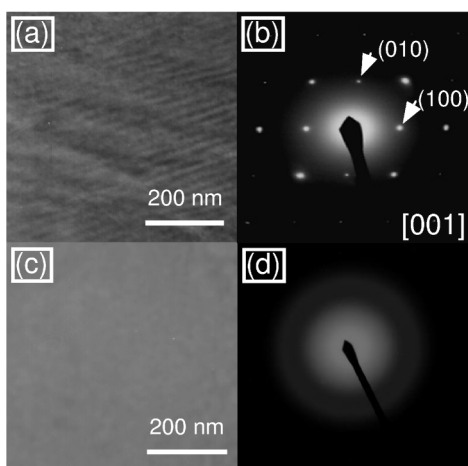
FIG. 6   Structural characterization of NBMN-pDA films. Before switching (nonconducting): (a) TEM, (b) diffraction. After switching (conducting): (c) TEM, (d) diffraction.

NBMN-pDA crystalline organic complex on the nanometer scale, and the transition can be reversed by the application of reverse pulses for a longer duration. An analysis of several possible mechanisms suggests that the conductance transition arises from the electric field pulse inducing local disorder into the crystalline thin film.

[1] T. Nakamura, T. Akutagawa, K. Honda, A. E. Underhill, A. T. Coomber, and R. H. Friend, Nature (London) **394**, 159 (1998); F. Zwick, D. Jerome, G. Margaritondo, M. Onellion, J. Voit, and M. Grioni, Phys. Rev. Lett. **81**, 2974 (1998); T. Kawamura, Y. Miyazaki, and M. Sorai, Chem. Phys. Lett. **273**, 435 (1997); H. Sirringhaus, N. Tessler, and R. H. Friend, Science **280**, 1741 (1998); A. Köhler, D. A. dos Santos, D. Beljonne, Z. Shuai, J.-L. Brédas, A. B. Holmes, A. Kraus, K. Müllen, and R. H. Friend, Nature (London) **392**, 903 (1998); J. M. Williams, A. J. Schultz, U. Geiser, K. D. Carlson, A. M. Kini, H. H. Wang, W.-K. Kwok, M.-H. Whangbo, and J. E. Schirber, Science **252**, 1501 (1991); D. Jéerome, Science **252**, 1509 (1991); G. Yu, J. Gao, J. C. Hummelen, F. Wudl, and A. J. Heeger, Science **270**, 1789 (1995); Y. Yang and A. J. Heeger, Nature (London) **372**, 344 (1994); G. M. Whitesides, J. P. Mathias, and C. T. Seto, Science **254**, 1312 (1991); M. C. Lonergan, Science **278**, 2103 (1997); M. Strukelj, F. Papadimitrakopoulos, T. M. Miller, and L. J. Rothberg, Science **267**, 1969 (1995).

[2] A. Aviram and M. A. Ratner, Chem. Phys. Lett. **29**, 277 (1974); A. Aviram and P. E. Seiden, U.S. Patent No. 3 953 874 (1976).

[3] A. Aviram, C. Joachim, and M. Pomerantz, Chem. Phys. Lett. **146**, 490 (1988).

[4] A. Aviram, C. Joachim, and M. Pomerantz, Chem. Phys. Lett. **162**, 416 (1989).

[5] R. S. Potember, T. O. Poehler, and D. O. Cowan, Appl. Phys. Lett. **34**, 405 (1979); R. S. Potember, T. O. Poehler, and R. C. Benson, Appl. Phys. Lett. **41**, 548 (1982); R. S. Potember, T. O. Poehler, A. Rappa, D. O. Cowan, and A. N. Bloch, Synth. Met. **4**, 371 (1982); R. S. Potember, T. O. Poehler, A. Rappa, D. O. Cowan, and A. N. Bloch, J. Am. Chem. Soc. **102**, 3659 (1980); R. S. Potember, T. O. Poehler, D. O. Cowan, F. L. Carter, and P. Brant, *Molecular Electronic Devices,* edited by F. L. Carter (Marcel Dekker, New York, 1983), p. 73; S. Yamaguchi and R. S. Potember, Mol. Cryst. Liq. Cryst. **267**, 241 (1995).

[6] B. B. Corson and R. W. Stoughton, J. Am. Chem. Soc. **50**, 2825 (1928).

[7] S. F. Alvarado, P. F. Seidler, D. G. Lidzey, and D. D. C. Bradley, Phys. Rev. Lett. **81**, 1082 (1998).

[8] L. P. Ma, W. J. Yang, Z. Q. Xue, and S. J. Pang, App. Phys. Lett. **73**, 850 (1998).

[9] C. Joachim and J. P. Launay, J. Mol. Electron. **6**, 37 (1990).

[10] M. P. Samanta, W. Tian, S. Datta, J. I. Henderson, and C. P. Kubiak, Phys. Rev. B. **53**, R7626 (1996).

[11] Hartree-Fock self-consistent field calculations, geometry optimizations, and harmonic vibrational analysis carried out with the code GAMESS: M. W. Schmidt, K. K. Baldridge, J. A. Boatz, S. T. Elbert, M. S. Gordon, J. H. Jensen, S. Koseki, N. Matsunaga, K. A. Nguyen, S. J. Su, T. L. Windus, M. Dupuis, and J. A. Montgomery, J. Comput. Chem. **14**, 1347 (1993). Original program assembled by M. Dupuis, D. Spangler, and J. J. Wendoloski. Polarized double-zeta (3-21G*) basis used for all atoms: J. S. Binkley, J. A. Pople, and W. J. Hehre, J. Am. Chem. Soc. **102**, 939 (1980); W. J. Pietro, M. M. Francl, W. J. Hehre, D. J. DeFrees, J. A. Pople, and J. S. Binkley, J. Am. Chem. Soc. **104**, 5039 (1982).

[12] K. Sohlberg, B. L. Baker, S. P. Leary, N. L. Owen, J. C. Facelli, and B. A. Trofimov, J. Mole. Struct. **354**, 55 (1995); K. Sohlberg, S. Leary, N. L. Owen, and B. Trofimov, Vib. Spectrosc. **13**, 227 (1997).

[13] As is conventional, HF-SCF frequencies were scaled ×0.89: M. Diem, *Introduction to Modern Vibrational Spectroscopy* (Wiley, New York, 1993).